Ferromagnetism of Anderson localized electrons: Application to cluster compounds

Subhalakshmi Lamba, Ashok K. Rastogi, and Deepak Kumar
School of Physical Sciences, Jawaharlal Nehru University, New Delhi, India 110067
(Received 6 January 1997)

A study of the electrical transport and magnetic properties of a series of cluster compounds with the generic formula $A_{0.5}M_2X_4$ suggests that the electrons at the Fermi surface are localized, and the ferromagnetism seen in these compounds arises from these electrons. The magnetism of these compounds shows some features characteristic of itinerant models and others which are characteristic of localized models. We construct a model which has a nondegenerate band of localized states with on-site repulsion. Further, the singly occupied states interact via direct exchange interaction which is ferromagnetic. Using a mean-field approximation we calculate the various magnetic properties, which are in qualitative accord with the observed behavior. In particular, we find that the single-particle excitations play a dominant role in the magnetism of these compounds, even though the electrons are localized. We also analyze the spin-wave excitations in this model and discuss their effect on low-temperature thermodynamics. [S0163-1829(97)01330-1]

I. INTRODUCTION

The transition metal cluster compounds of the family $A_{0.5}M_2\ X_4$ (where A is Ga or Al, M is one of the transition metals V or Mo, and X is S, Se, or Te) exhibit very interesting ferromagnetic behavior which is a curious mixture of itinerant and localized behavior.[1,2] These compounds have a spinel structure with a reduction of the space group symmetry from $Fd3m$ to $F\overline{4}3m$ and half occupancy of the cation A sites.[3,4] These are termed cluster compounds, because there is a significant clustering of the transition metals into tetrahedral clusters, with intercluster distances between M ions much larger ($\geqslant 4$ Å) than the intracluster distances of 3 Å, which are in the metallic range.[3,4]

The conductivity of these compounds, both dc and ac, has the classic signature of variable-range hopping over a wide temperature range ($<200^0$ K),[5,6] which implies that there is a finite density of localized states at the Fermi level. On the other hand these compounds seem to have a rather weak disorder, which is not discernible in x-ray diffraction studies. The possible reasons for the electron localization are discussed in the next section. These compounds are also ferromagnetic with transition temperatures in the range of 10 K to 26 K.[7] The specific heat exhibits a large linear contribution in the paramagnetic regime and in the ferromagnetic regime a weak $T^{3/2}$ contribution in addition to a reduced linear contribution.[7,8] The magnetic contribution to the specific heat shows a jump at the transition temperature, a behavior typical to itinerant ferromagnets. The spontaneous magnetization as seen in the M vs H curves corresponds to nonintegral moments, but the high field saturation magnetization corresponds to a magnetization of a single electron per cluster. Similarly the moment inferred from the high-temperature susceptibility measurements is different from the spontaneous moment. However, the Arrott plots (M^2 vs H/M) show a pronounced curvature even at small fields, which is in contrast to the itinerant behavior.[7,8]

All this points to the fact that the single-particle excitations in the system play a dominant role in the magnetic behavior. Though the electrons are not itinerant in the system, there is a finite density of states at the Fermi level, and hence the possibility of low energy charge excitations. This indicates that the magnetic properties also originate from this band of localized electrons, and the itinerantlike features of magnetism then come from the low energy electronic excitations across the Fermi level. Accordingly, in this paper, we investigate the magnetic properties of a model in which the electrons are Anderson localized. The magnetic moment in the model arises due to the fact that part of the band around the Fermi level is singly occupied due to on-site Coulomb repulsion U, whose magnitude relative to the bandwidth $2W$ has to be chosen keeping in mind that every transition metal cluster contributes the same number of electrons ($n=1$) to the magnetic moment and the single-particle excitations have no gap. The magnetic moments of the singly occupied sites then interact ferromagnetically via direct exchange. This situation is particularly favorable for the mechanism of direct exchange, as the electrons occupy localized states that are mutually orthogonal to each other. With these inputs, we find that the model exhibits most of the aforementioned features of magnetism. To get qualitative agreement, we attempt to obtain a typical set of values of the parameters U,W and the direct exchange energy J, for one of these compounds. A paramagnetic version of this model (without the exchange interaction J) was investigated earlier by Kaplan, Mohanti, and Hartman (KMH).[9] This study showed that the magnetic susceptibility of the model has both Curie behavior and Pauli behavior. The paramagnetism of Anderson localized states and other properties like specific heat, have also been studied in detail by Kamimura and co-workers,[10,11] especially in the context of phosphorus-doped silicon.

The rest of the paper is organized as follows. In the next section, we describe the model and its justification for the magnetism of cluster compounds. In Sec. III, we investigate the model in a self-consistent mean-field approximation. Within this approximation this model already exhibits a rich physical behavior. We present results on various thermodynamic properties. In Sec. IV, we go beyond the mean-field

approximation by using a functional variational method which is equivalent to a self-consistent renormalized high density expansion. Though we have the formal results, our analysis is done to understand the role of spin-wave excitations at low temperatures, as these were missed out in the mean-field analysis. We end the paper with a discussion and summary of our results in the concluding section. A discussion on the chemical potential and most of the details of the functional method are discussed in two appendices.

II. MODEL AND PRELIMINARY DISCUSSION

In order to make the discussion concrete, we consider the specific case of one particular cluster compound, GaV_4S_8. A simple valence count, keeping in mind that Ga is trivalent and S is divalent, shows that three of the V atoms in the formula unit must be trivalent and one must be tetravalent. This suggests that the Fermi level should lie within the d bands of the V atom. The preliminary band structure calculations,[12] indeed show that the band character at the Fermi level is dominantly d type.[12] Two other features of note are that the bands at the Fermi level are very narrow and they each seem to disperse only along one family of crystallographic directions. This suggests a tight binding picture of t_{2g}-like bands in which each of the degenerate levels in a cluster disperses by having overlaps in one direction only. The narrowness and quasi-one-dimensional character of the bands makes it easy for these electrons to become localized with very weak disorder. This weak disorder may arise either due to the occupancy of Ga ions which occupy only half of the A sites of the spinel structure or due to possible charge disorder of V^{3+} and V^{4+} ions among tetrahedral clusters. Taking these features into account we model the system by considering a localized band of electrons with one electron per cluster site. The localization length estimated from the transport data suggests that electrons are localized almost within each cluster.[5]

The two most relevant interactions for our purpose are (a) the on site Coulomb interaction U, and (b) the direct ferromagnetic exchange, $J(R)$, between singly occupied sites. For such a localized system, the long range Coulomb Interaction should also be considered. The main physical consequence of the long range part of the interaction is that the single-site energies have site-occupation-dependent Hartree contributions. In an average picture this has two implications. First there is an increase in the bandwidth, W, due to an additional spread of the Hartree energies. Second there is a depletion in the density of states at the Fermi level, $g(\epsilon_F)$. In the following considerations we do not treat these effects, rather we take them as included in parameters adjustable from derived magnetic properties.

There are two further comments in order here. First the on-site interaction parameter U is dependent on the localized state i, as has been considered by Kamimura.[10] Here, however, we ignore the state dependence of U, as we are working in the regime of deeply localized states (with an activation energy $\epsilon_{\rm act} \simeq 0.2$ eV), whose localization length is very small. It would not have been possible to ignore the state dependence of U if one was working near the mobility edge. Our second remark is concerned with magnetic interactions. The intersite Coulomb interactions also allow for the kinetic exchange,[13] which is antiferromagnetic. Since the compounds we are dealing with are ferromagnetic,[14] the direct exchange dominates, but the interaction constant $J(R)$ should be interpreted as the sum of the direct and the kinetic exchange.

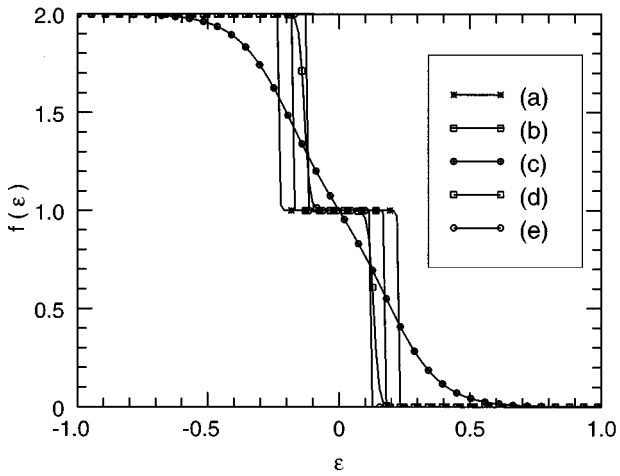

FIG. 1. Variation of the occupation function $f(\epsilon)$ with energy ϵ for $U/W=0.25$, at different temperatures T and magnetic field h, where ϵ is in units of W, T is in units of W/k_B, and h is in units of $W/g\mu_B$ for (a) $T=0.001, h=0.2$; (b) $T=0.001, h=0.1$; (c) $T=0.1, h=0$; (d) $T=0.01, h=0$; and (e) $T=0, h=0$. At $T=0$ the steps are from $f(\epsilon)=2$ to $f(\epsilon)=1$, at $\epsilon=\mu-U$ and from $f(\epsilon)=1$ to $f(\epsilon)=0$ at $\epsilon=\mu$, the width of singly occupied bands $[f(\epsilon)=1]$ increases with h.

With these assumptions, the Hamiltonian of the model in the presence of an external magnetic field can be written as,

$$H=\sum_i \epsilon_i(n_{i\uparrow}+n_{i\downarrow})+\sum_i Un_{i\uparrow}n_{i\downarrow}-\frac{1}{2}\sum_{ij} J_{ij}\vec{S}_i\cdot\vec{S}_j$$

$$-g\mu_B H_e\sum_i S_i^z, \tag{1}$$

where i labels the localized states and ϵ_i are the energies of the localized states that form a band of width $2W$. Since the localization radius of these states is of the same order as the cluster size, we take i to label the cluster. The spin operators $\vec{S}_i$ are, as usual, represented as

$$\vec{S}_i=\tfrac{1}{2}c_{i\alpha}^{\dagger}\vec{\sigma}_{\alpha\beta}c_{i\beta}, \tag{2}$$

where $\vec{\sigma}$ are the Pauli spin matrices and $c_{i\alpha}^{\dagger}$ ($c_{i\alpha}$) are the creation (annihilation) operators for the electrons, $J_{ij}=J(R_{ij})$, R_{ij} being the separation between the sites i and j and H_e the external magnetic field. In order to appreciate the role of U and to fix its magnitude, it is instructive to first study the model without the exchange interaction, which is the model considered by KMH.[9] When $U=0$, in the ground state half the sites are doubly occupied and the other half are empty, with the Fermi level being at the center of the band (assuming the density of states to be symmetric about the center). In this situation there can be no magnetic moment. In the other extreme when $U \gg W$, all the sites are singly occupied, and the single-particle excitations have the Mott-Hubbard gap as usual. Since these compounds exhibit ferro-

magnetism and hopping conduction, which requires a finite density of states at the Fermi level, neither of the above situations describe the physics of the problem. If $U<W$, KMH (Ref. 9) showed that the low lying states will be doubly occupied, a fraction of states covering the energy U around the Fermi level will be singly occupied and the rest of the higher energy states will be empty. The singly occupied states are responsible for magnetic properties and give rise to the ferromagnetic behavior when the exchange term is included. Note that the KMH model is soluble as it breaks up into individual site Hamiltonians. It is simple to calculate the grand canonical free energy and the occupation function f_i. These expressions are

$$G=-k_BT\sum_i \ln\left(1+2\cosh\frac{\beta h}{2}e^{-\beta(\epsilon_i-\mu)}+e^{-\beta(2\epsilon_i+U-2\mu)}\right), \tag{3}$$

$$f_i=2\left[\frac{\cosh(\beta h/2)e^{-\beta(\epsilon_i-\mu)}+e^{-\beta(2\epsilon_i+U-2\mu)}}{[1+2e^{-\beta(\epsilon_i-\mu)}\cosh(\beta h/2)+e^{-\beta(2\epsilon_i+U-2\mu)}]},\right] \tag{4a}$$

$$n=\frac{N}{\mathcal{N}_0}=\frac{2}{\mathcal{N}_0}\int_{-W}^{W}d\epsilon g(\epsilon) \times\left[\frac{\cosh\frac{\beta h}{2}\,e^{-\beta(\epsilon-\mu)}+e^{-\beta(2\epsilon+U-2\mu)}}{1+2e^{-\beta(\epsilon-\mu)}\cosh\frac{\beta h}{2}+e^{-\beta(2\epsilon+U-2\mu)}}\right] \tag{4b}$$

where μ is the chemical potential, $\mathcal{N}_0$ is the total number of clusters, and h is $g\mu_BH_e$. In writing Eq. (4b) we have introduced the density of states $g(\epsilon)$ and taken the zero of the energy to be the center of the band. We further restrict ourselves only to a symmetric density of states, i.e., $g(\epsilon)=g(-\epsilon)$. In this situation, for the case of $n=1$, the chemical potential μ can be exactly obtained to be $U/2$ at all temperatures (see Appendix A). In Fig. 1 we exhibit the occupation function f_i for different temperatures and fields. For the zero-field ground state, levels $\epsilon_i<\mu-U$ are doubly occupied, levels between $\mu-U<\epsilon_i<\mu$ are singly occupied, and levels $\epsilon_i>\mu$ are unoccupied. Thus there are two steps across which single-particle excitations can occur as one sees in the finite temperature curves. As mentioned above the magnetic moment is contributed by the singly occupied sites which range over an energy of U. In the presence of a magnetic field h, at $T=0$ the steps basically occur at $\mu-U-h/2$ from doubly to singly occupied sites which all have up spin and at $\mu+h/2$ from singly occupied to unoccupied. We further note that the low energy single-particle excitations involve hops between states that may be well separated in space. Thus the equilibration rates for such systems, that depend upon phonon-assisted hopping, may be low, at low temperatures.

III. MEAN-FIELD APPROXIMATION

Due to the presence of the exchange term, the Hamiltonian of Eq. (1) is not site separable and its partition function cannot be obtained exactly. In this section, we examine the problem in the site averaged mean-field approximation (MFA). This already leads to many new nontrivial results, which bear good comparisons with experimental behavior. As usual, in MFA, the exchange term is written as

$$\frac{1}{2}\sum_{ij} J_{ij}\vec{S}_i\cdot\vec{S}_j=\sum_{i,j} J_{ij}\left(m_jS_i^z-\frac{1}{2}m_im_j\right), \tag{5}$$

where m_i denotes the thermal average $\langle S_i^z\rangle$ to be determined self-consistently. This leads to the following site-separable Hamiltonian:

$$H_{\rm MF}=\sum_{i=1}^{\mathcal{N}_0}\left[\left(\epsilon_i-\frac{h+I_i}{2}\right)n_{i\uparrow}+\left(\epsilon_i+\frac{h+I_i}{2}\right)n_{i\downarrow}+Un_{i\uparrow}n_{i\downarrow}\right] +\frac{1}{2}\sum_{ij} J_{ij}m_im_j, \tag{6}$$

where I_i denotes the local internal field $\Sigma_jJ(R_{ij})m_j$. It should be noted that the local field is contributed by only singly occupied sites, whose density is of the order $(U/2W)n_s$, where n_s is the density of sites. Thus the nearest neighbor distance is of the order of $(2W/Un_s)^{1/3}$, which must be kept in mind while estimating the internal fields I_i. One can now straightforwardly obtain the expression for electron number per site n, local magnetization m_i, and the internal energy E:

$$n=\frac{2}{\mathcal{N}_0}\sum_i\left(\cosh\frac{\beta}{2}(h+I_i)+\exp[-\beta(\epsilon_i+U-\mu)]\right) \times\frac{e^{-\beta(\epsilon_i-\mu)}}{\mathcal{Z}_i}, \tag{7}$$

$$m_i=\sinh\frac{\beta}{2}(h+I_i)\frac{e^{-\beta(\epsilon_i-\mu)}}{\mathcal{Z}_i}, \tag{8}$$

$$E=\sum_i\left\{2(\epsilon_i-\mu)\cosh\frac{\beta}{2}(h+I_i)-(h+I_i)\sinh\frac{\beta}{2}(h+I_i) +(2\epsilon_i+U-2\mu)\exp[-\beta(\epsilon_i+U-\mu)]\right\} \times\frac{e^{-\beta(\epsilon_i-\mu)}}{\mathcal{Z}_i}+\frac{1}{2}\sum_{ij} J_{ij}m_im_j, \tag{9}$$

where we define $\mathcal{Z}_i$ as

$$\mathcal{Z}_i=1+2\cosh\frac{\beta}{2}(h+I_i)\exp[-\beta(\epsilon_i-\mu)] +\exp[-\beta(2\epsilon_i+U-2\mu)]. \tag{10}$$

Though the above set of equations involve site-dependent quantities, which can only be solved numerically, it should be realized that the problem has actually rather slight positional disorder. Further since we are dealing with a high density ferromagnet, it seems very reasonable to assume that the magnetization and the local field are homogenous with little local fluctuation. The magnetization equation for site-averaged magnetization $m=(1/\mathcal{N}_0)\Sigma_im_i$ can be written as

$$m=\int_{-W}^{W} d\epsilon g(\epsilon) \times\left[\frac{\sinh(\beta/2(h+J_0m))}{e^{\beta(\epsilon-\mu)}+2\cosh(\beta/2(h+J_0m))+e^{-\beta(\epsilon-\mu+U)}}\right], \tag{11}$$

where we have written the average value of I as J_0m. Equation (7) is to be used for the determination of μ, which as shown in Appendix A is found to be $U/2$ for a half-filled band.

A. Analytical results

Before proceeding with the general analysis of Eq. (11), we present the case of a uniform density of states: $g(\epsilon)=1/2W$, as the integral can then be exactly evaluated to yield

$$m=\frac{\sinh(\beta/2(h+J_0m))e^{\beta U/2}}{2\beta W}\frac{1}{\sqrt{\alpha^2-1}}\ln\left[\frac{e^{\beta W}+\alpha-\sqrt{\alpha^2-1}}{e^{\beta W}+\alpha+\sqrt{\alpha^2-1}} \times\frac{1+\alpha+\sqrt{\alpha^2-1}}{1+\alpha-\sqrt{\alpha^2-1}}\right] \tag{12}$$

with

$$\alpha=e^{\beta U/2}\cosh\frac{\beta}{2}(h+J_0m). \tag{13}$$

We now use Eq. (12) for calculating various magnetic properties. The susceptibility in the paramagnetic phase is found to be

$$\chi=\mathcal{N}_0(g\mu_B)^2\frac{\chi_0}{1-J_0\chi_0} \tag{14}$$

with

$$\chi_0=\frac{1}{8W(1-e^{-\beta U})^{1/2}} \times\ln\left[\frac{1+(\alpha\cosh\beta W+\sqrt{\alpha^2-1}\sinh\beta W)}{1+(\alpha\cosh\beta W-\sqrt{\alpha^2-1}\sinh\beta W)}\right]. \tag{15}$$

In the interesting temperature range $\beta W>\beta U\gg 1$,

$$\chi_0\sim\left(\frac{\ln 4}{8W}+\frac{U}{8Wk_BT}\right). \tag{16}$$

This result was obtained by KMH, (Ref. 9) and shows the features of Curie behavior due to moments and a Pauli-type term due to single-particle excitations. In our case, the susceptibility assumes the form

$$\chi=\mathcal{N}_0(g\mu_B)^2\frac{C+C_1T}{k_B(T-T_C)}, \tag{17}$$

where the Curie temperature T_c is given by

$$k_BT_C=\frac{UJ_0}{8W-J_0\ln 4}\simeq\frac{1}{4}UJ_0g(\epsilon_F) \tag{18}$$

and C and C_1 are given by

$$C=\frac{U}{8W-J_0\ln 4}, \tag{19}$$

$$C_1=\frac{k_B\ln 4}{8W-J_0\ln 4}. \tag{20}$$

To shed more light on this expression we calculate the spontaneous magnetization $m_s(0)$ at zero temperature to be (in units of $g\mu_B$)

$$m_s(0)\simeq\frac{U}{4W-2J_0}. \tag{21}$$

Recalling the discussion of the Sec. II, we see that the spontaneous magnetization is nearly the same as the number of singly occupied sites. Note that the constant C is not simply related to $m_S(0)$, which would have been the case for a localized model. Further, from the form of Eq. (17), one sees that the effective Curie constant shows a slight increase with temperature, which is a consequence of single-particle excitations. Next, we calculate the saturation magnetization which is easily calculated from Eq. (12) by taking the $h\to\infty$ limit and is found to be $0.5g\mu_B$, which is again quite different from the spontaneous magnetization $m_s(0)$. Finally it is worth making a remark about the expression for T_C. It involves both the interaction constants U and J_0. $Ug(\epsilon_F)$ roughly determines the zero-temperature spontaneous magnetization and J_0 the coupling strength of the internal magnetization.

The results of the calculations with a constant DOS may miss some of the important physical features, so we now present the results of the analysis with a more general, symmetric DOS. We first analyze the spontaneous magnetization in the $T\to 0$ limit. In this limit Eq. (11) can be written as

$$m_s=\frac{1}{2}\int_{-W}^{W} d\epsilon g(\epsilon)\left[\frac{1}{e^{\beta(\epsilon-U/2-J_0m/2)}+1+e^{-\beta(\epsilon+U/2+J_0m/2)}}\right]. \tag{22}$$

Here we have dropped terms of the order of $(e^{-\beta J_0m/2})$. As $\beta\to\infty$, the integrand $\mathcal{I}$ has the following behavior;

$$\begin{aligned}\mathcal{I}&=0, \quad \epsilon>(U+J_0m)/2\\ &=1, \quad (U+J_0m)/2\geqslant\epsilon\geqslant-(U+J_0m)/2\\ &=0, \quad \epsilon<-(U/2+J_0m)/2.\end{aligned} \tag{23}$$

Thus we obtain

$$m_s(0)=\frac{1}{2}\int_{-(U+J_0m)/2}^{(U+J_0m)/2} d\epsilon g(\epsilon) =\frac{1}{2}\left[\mathcal{N}\left(\frac{U+J_0m}{2}\right)-\mathcal{N}\left(-\frac{U+J_0m}{2}\right)\right], \tag{24}$$

where $\mathcal{N}(\epsilon)$ is the integrated density of states,

$$\mathcal{N}(\epsilon)=\int_{-W}^{\epsilon} d(\epsilon)g(\epsilon). \tag{25}$$

For a constant DOS, Eq. (24) yields the same results as Eq. (21). It can be easily solved for the case of weak magnetization, that is $m_s(0) \ll 1$

$$m_s(0) = \frac{\mathcal{N}(U/2) - \mathcal{N}(-U/2)}{2\{1-(J_0/4)[g(U/2)+g(-U/2)]\}}. \quad (26)$$

Next we consider the susceptibility in the paramagnetic regime. For this we write Eq. (11) in the following form:

$$m = \frac{1}{2}\int_{-W}^{W} d\epsilon g(\epsilon) \frac{e^{\beta(h+J_0 m)/2} - e^{-\beta(h+J_0 m)/2}}{e^{\beta(\epsilon-U/2)} + e^{\beta(h+J_0 m)/2} + e^{-\beta(h+J_0 m)/2} + e^{-\beta(\epsilon+U/2)}} = \frac{1}{2}(n_\uparrow - n_\downarrow) \quad (27)$$

and

$$n_\uparrow = \int d\epsilon \frac{g(\epsilon)}{1 + e^{-\beta(h+J_0 m)} + e^{\beta\left(\epsilon - \frac{U+h+J_0 m}{2}\right)} + e^{\beta\left(\epsilon + \frac{U+h+J_0 m}{2}\right)}} \quad (28)$$

Again for large β ($T > T_C, k_B T \ll U < W$) the integrand has a nonzero value $[1+\exp -\beta(h+J_0 m)/2]$ only when

$$-\frac{U+h+J_0 m}{2} < \epsilon < \frac{U+h+J_0 m}{2}$$

and is zero otherwise. Thus

$$n_\uparrow = \frac{1}{1+\exp(-\beta(h+J_0 m)/2)} \times \left\{ \mathcal{N}\left(\frac{U+h+J_0 m}{2}\right) - \mathcal{N}\left(-\frac{U+h+J_0 m}{2}\right)\right\}. \quad (29)$$

A similar analysis for $n_\downarrow$ yields

$$n_\downarrow = \frac{1}{1+\exp(\beta(h+J_0 m)/2)} \times \left\{ \mathcal{N}\left(\frac{U-h-J_0 m}{2}\right) - \mathcal{N}\left(-\frac{U-h-J_0 m}{2}\right)\right\}. \quad (30)$$

From these expressions the susceptibility is easily obtained in the same form as in Eq. (14), with χ_0 given by

$$\chi_0 = \frac{1}{k_B T}[\mathcal{N}(U/2) - \mathcal{N}(-U/2)] + [g(U/2) + g(-U/2)] \quad (31)$$

which is the generalization of Eq. (16). It is worth remarking that in the above results the DOS at $U/2$ and $-U/2$ occur, as these are the points of discontinuity of the occupation function when the magnetization $m=0$. The large field case can also be analyzed for a general DOS. From the earlier discussion it is clear that the singly occupied sites that are aligned to the field lie in the energy range $(U+h+J_0 m)/2 \geq \epsilon \geq -(U+h+J_0 m)/2$. For a sufficiently large magnetic field h, this would cover the entire band, yielding a saturation magnetization of $0.5 g\mu_B$. It might be thought that a generalized version of the Sommerfeld expansion may be developed but our efforts in those directions have not been successful.

B. Numerical results

We now present some numerical results for various thermodynamic quantities, within the mean-field approximation. We again work with a symmetric density of states, in which case the chemical potential is fixed to be $U/2$, for a half-filled band. These restrictions do make the analysis simpler, but the general results are quite representative. Our analysis is done for the following density of states, which is rather typical:

$$g(\epsilon) = \frac{2}{\pi W^2}\sqrt{W^2 - \epsilon^2}, \quad -W \leq \epsilon \leq W. \quad (32)$$

Most of the results presented are for the specific value of $U/W = 0.25$, and for $J_0/W = 0.1$ and 0.2, though variations with U and J_0 have also been examined. We have chosen the value of W to be 1 eV.

The spontaneous magnetization in the $T \to 0$ limit can be directly evaluated from Eq. (24), which for the density of states Eq. (32) is

$$m_s(0) = \frac{1}{\pi}[\sin^{-1} x + x\sqrt{1-x^2}], \quad (33)$$

where $x = [U + J_0 m_s(0)]/2W$. We plot the solutions of this equation for different values of U/W over a range of J_0/W in Fig. 2. One notes that the value of $m_s(0)$ depends mainly on U, which as mentioned earlier controls the number of singly occupied states in the occupied band and is not much influenced by the choice of J_0/W and it is always less than the high field saturation magnetization of $0.5 g\mu_B$.

The critical temperature T_C where the spontaneous magnetization becomes zero can be determined from the equation

$$k_B T_C = J_0 \int_0^W d\epsilon g(\epsilon)[e^{\beta_C(\epsilon - U/2)} + 2 + e^{-\beta_C(\epsilon + U/2)}]^{-1}, \quad (34)$$

where $\beta_C = 1/(k_B T_C)$. The variation of the temperature T_C with U/W and J_0/W is shown in Fig. 3 which compares well with the approximate solutions of Eq. (18).

The general variation of the spontaneous magnetization $m_s(T)$ with temperature, can be studied from the $h \to 0$ limit

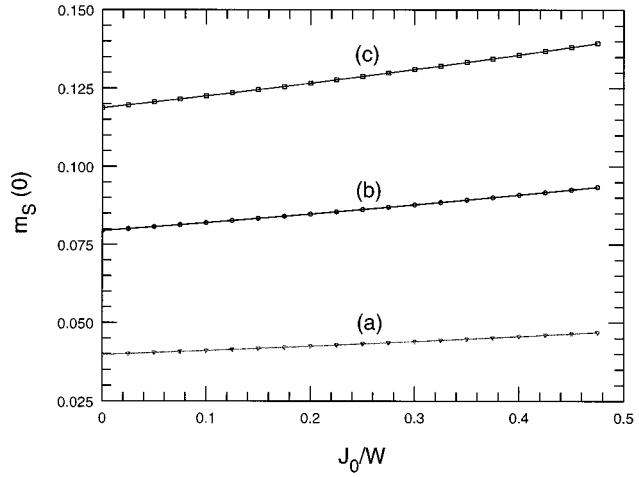

FIG. 2. Variation of the spontaneous magnetization $m_s(0)$, measured in units of $g\mu_B$, with the exchange interaction J_0/W for (a) $U/W=0.125$, (b) $U/W=0.25$, and (c) $U/W=0.375$.

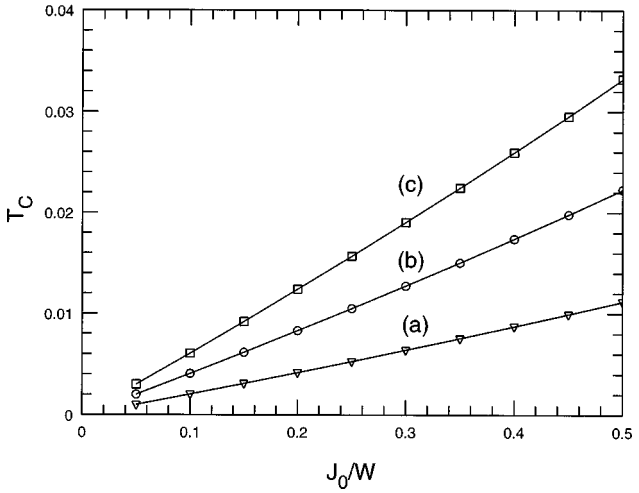

FIG. 3. Variation of the critical temperature T_C (in units of W/k_B) with J_0/W for (a) $U/W=0.125$, (b) $U/W=0.25$ and (c) $U/W=0.375$.

of Eq. (11). The typical plots for $m_s(T)$ are presented in Fig. 4. The high-temperature variation of $m_s(T)$ with temperature is typically mean-field like $[(T-T_C)^{1/2}]$. But to focus on the low-temperature behavior, a plot of $m_s(0)-m_s(T)$, is shown in the inset of Fig. 4. In this, no clear-cut variation like T^2 as expected from single-particle excitations in the band model or $\exp[-2J_0 m_s(T)/T]$ as expected in the localized model can be discerned.

We next consider the susceptibility in the paramagnetic phase. We first calculate χ_0 for the chosen density of states from the equation

$$\chi_0=\frac{\beta}{2}\int_{-W}^{W} d\epsilon g(\epsilon)\left[\frac{1}{e^{\beta(\epsilon-U/2)}+2+e^{-\beta(\epsilon+U/2)}}\right]. \quad (35)$$

χ_0 for a circular DOS has the same general features as for the uniform density of states [Eq. (16)], i.e., a combination of the $1/T$ behavior due to localized moments and the Pauli-like contribution from the single-particle excitations. We plot $\chi(T-T_C)$ [where χ is the enhanced susceptibility in the paramagnetic phase, given by Eq. (14)], with temperature in Fig. 5. We find that the effective Curie constant $C'(\chi\sim C'/T)$ actually increases with temperature, indicating that there is a contribution to the magnetization from the single-particle excitations accords the Fermi level. We fit the curves obtained to the general law Eq. (17). The values of both C and C_1 are different for the the different values of J_0/W, and $C\simeq 0.04$ is indeed smaller than the corresponding saturation magnetization. In Fig. 6 we plot the variation of the enhanced susceptibility with temperature, in the paramagnetic phase, for different values of the on-site Coulomb repulsion U/W for both a zero and nonzero J_0/W. The divergence in the curves for the nonzero J_0/W indicates the transition to the ferromagnetic phase.

In Fig. 7 we study the variation of the isothermal magnetization with the magnetic field from Eq. (11). The magnetization saturates to a value of $0.5g\mu_B$ at rather high fields $(h\sim 1)$. For $T=0$ the saturating field $h_{\rm sat}$ is in fact $\simeq 2W-U-2J_0$. Below the critical temperatures one notes that before saturation there is actually a large range of fields,

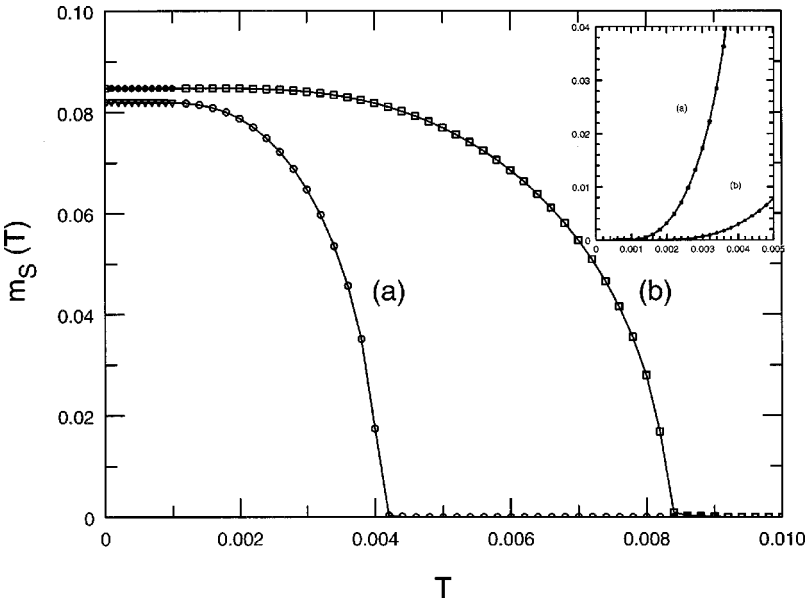

FIG. 4. Variation of the spontaneous magnetization $m_s(T)$, in units of $g\mu_B$ with temperature T for (a) $J_0/W=0.1$ and (b) $J_0/W=0.2$, the inset shows the corresponding variation of $m_s(0)-m_s(T)$ with temperature T for very low temperatures $T\ll T_C$, where T is measured in units of W/k_B.

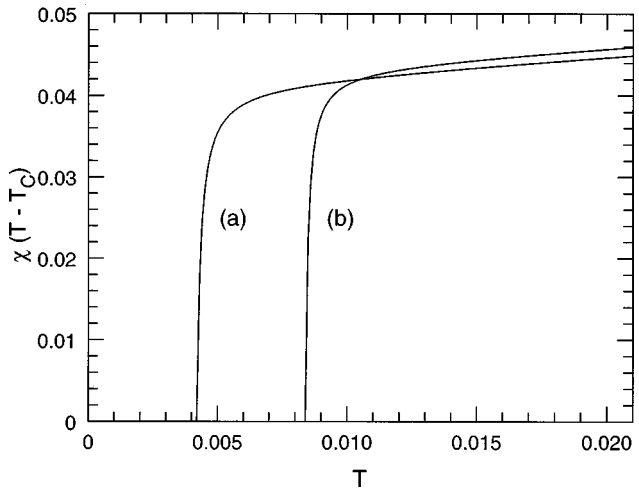

FIG. 5. Variation of the enhanced susceptibility $\chi(T-T_C)$ in the nonmagnetic phase, with temperature T. The best possible fit to the general form $\chi=(C+C_1T)/(T-T_C)$, gives us the values of C and C_1 to be (a) $J_0/W=0.1$, $C=0.0396$, and $C_1=0.254$ and for (b) $J_0/W=0.2$, $C=0.0401$, and $C_1=0.279$, the unit of χ being $W/(g\mu_B)^2$.

over which the magnetization increases linearly with the field strength. Above T_C also, after an initial nonlinear rise, the magnetization increases linearly with field over a considerable range of fields. These features are quite different from the localized model and are in accord with the high field magnetization behavior of the cluster compounds.

For any magnetic system the Arrott plots offer a useful insight into the type of magnetic behavior. We present the Arrott plots for this model in Fig. 8, for the density of states given in Eq. (32). The plots, which are over a large range of temperatures, both below and above T_C ($0.006<T<0.015$), show a large deviation from the linear behavior expected in weak itinerant ferromagnets like $ZrZn_2$ and Ni_xPt_{1-x}.[15] In such ferromagnets, the plots enable us to obtain the parameters of the Landau theory and the curvature of the Arrott plots is reflective of the shape of the density of states. In our model one can observe strong curvature even at

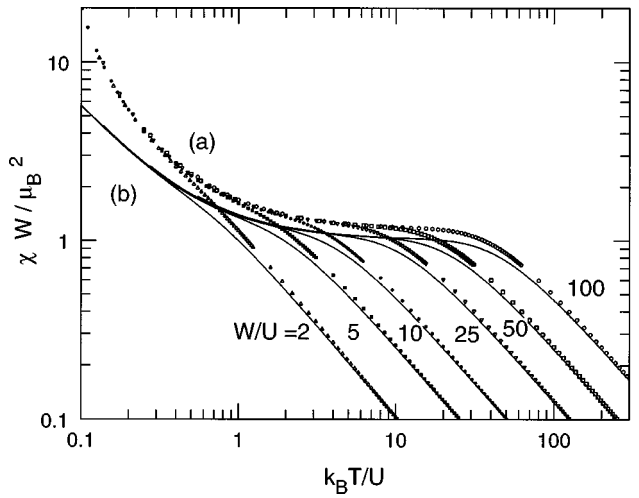

FIG. 6. Variation of the enhanced susceptibility χ with T/U in the paramagnetic phase for (a) $J_0/W=0.5$ and (b) $J_0/W=0$, for different strengths of U, the on-site Coulomb repulsion.

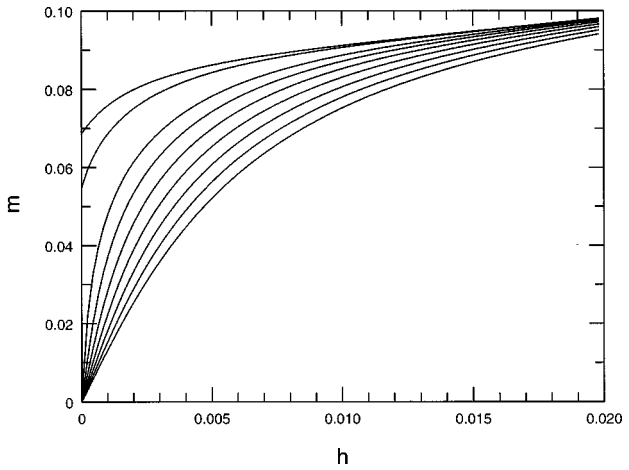

FIG. 7. Variation of isothermal magnetization $m(h)$ with magnetic field strength h, for different temperatures $0.006\leqslant T\leqslant 0.015$, with $J_0/W=0.2$, the magnetization saturates to 0.5, in units of $g\mu_B$, at very high fields ($h\simeq W$).

small fields. To understand this, we show in Fig. 9 the occupation function for up and down spins at two values of the field at a fixed temperature. From this, one sees how the magnetization which is related to the difference in the areas under the up-spin and down-spin curves changes nonlinearly. In contrast to the itinerant situation the nonlinearity, being rather strong, is not very dependent on the shape of the density of states. Only at higher temperatures the plots become almost parallel to each other, characteristic of typical itinerant ferromagnets. These plots bear a good resemblance to the experimental plots for the cluster compounds presented in (Ref. 8).

We calculate the zero-field specific heat in the ferro- and paramagnetic phases for the circular DOS for two different values of J_0/W. These are shown in Fig. 10. Note that the specific heat shows a huge jump just before the magnetic transition takes place. The magnitude of the jump ΔC seems to increase with the critical temperature, and also with J_0/W for a fixed value of U/W though we are unable to pinpoint an exact dependance with either T_C or $m_S(0)$. In the ferromagnetic phase the specific heat is quite distinct for dif-

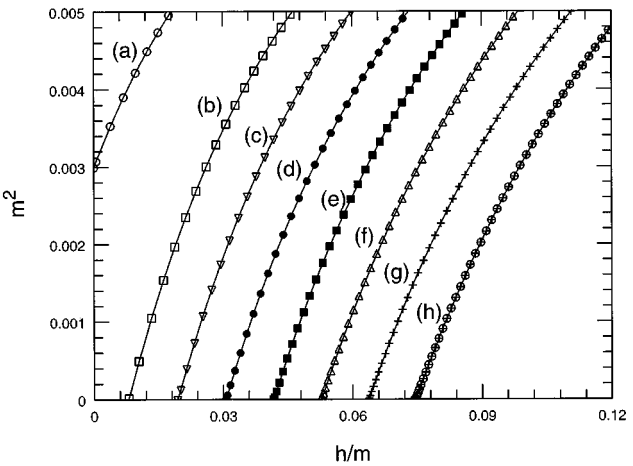

FIG. 8. Arrott plots for $J_0/W=0.2$, at temperatures (a) 0.007, (b) 0.009, (c) 0.01, (d) 0.011, (e) 0.012, (f) 0.013, (g) 0.014, and (h) 0.015 ,where T is k_BT/W.

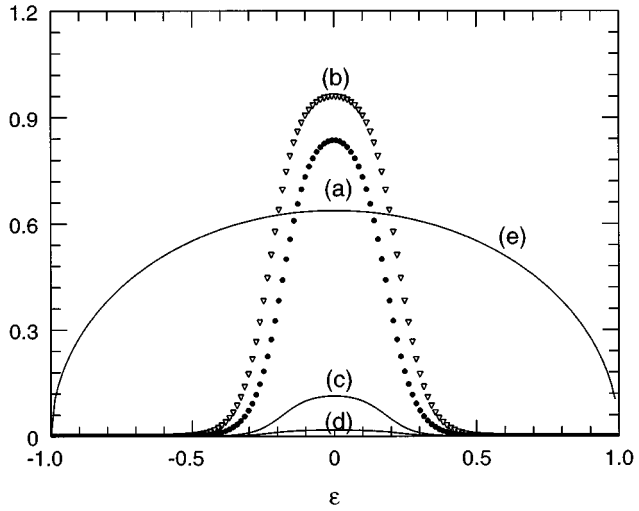

FIG. 9. Variation of the occupation function for the singly occupied sites with energy ϵ (in units of W) at a temperature of 0.05 (in units of W/k_B), for the up-spin band at (a) $h=0.1$ and (b) $h=0.2$ and for the down-spin band at (c) $h=0.1$ and (d) $h=0.2$ where h is the magnetic field, and finally, (e) the density of states, $g(\epsilon)$.

ferent values of the parameter J_0/W, but beyond the T_C the two curve merge to one, which is an artefact of the mean-field approximation. In both the para- and ferro-magnetic phases the specific heat is found to be linear in temperature, over a wide range of temperature $C_V=\gamma T$ with γ dependant on the shape of the density of states studied and in the ferromagnetic phase on the value of J_0/W. This feature is also in accord with the experimental observations.

IV. BEYOND MEAN-FIELD THEORY

The mean-field approximation discussed above is inadequate in many respects. Being a single-site approximation, it misses the correct low energy magnetic excitations which are cooperative spin waves. It also cannot give an account of magnetic correlations between different sites. Moreover in this model one also has to consider the interaction between spin excitations and particle excitations. Since the analysis of these problems is a difficult exercise, in this section we confine ourselves to the inclusion of spin-wave excitations. We do this by developing a version of renormalized high density expansion,[16,17] by using a functional method combined with a variational technique.[18,19] Such methods have been used in a number of similar quantum statistical problems. For the present calculation, as far as longitudinal degrees of freedom are concerned, the results are equivalent to the self-consistent high density expansion to first order, while the transverse degrees of freedom are treated to include spin-wave contributions to the leading order.[19] Since the techniques used are available in literature, in this section we outline the main steps and approximations, relegating the details of the derivation to Appendix B.

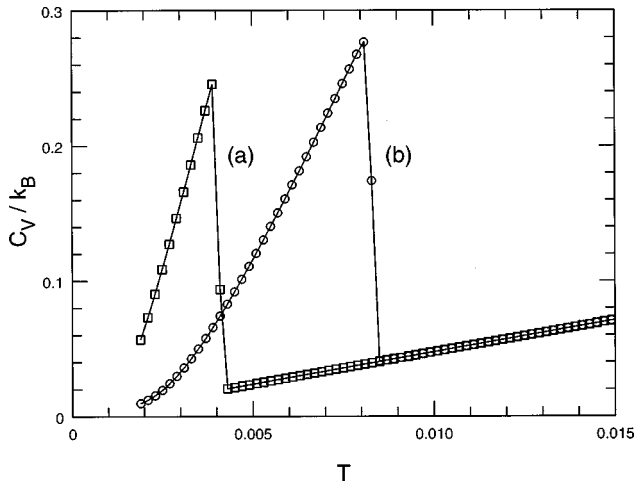

FIG. 10. Variation of the specific heat C_V with temperature for (a) $J_0/W=0.1$ and (b) $J_0/W=0.2$. γ in the paramagnetic phase is estimated from this to be 3.5 mJ/mol K^2, the specific heat shows a huge jump at the onset of the magnetic transition.

Since the Hamiltonian involves noncommuting variables, the grand canonical partition function $Z_G=\exp[-G(T,\mu,h)]$ is written as

$$Z_G=\mathrm{Tr}T\left[\exp\left\{-\int_0^\beta d\tau\sum_i\left[\tilde{\epsilon}_{i\uparrow}n_{i\uparrow}(\tau)+\tilde{\epsilon}_{i\downarrow}n_{i\downarrow}(\tau)+Un_{i\uparrow}(\tau)n_{i\downarrow}(\tau)\right]-\frac{1}{2}\sum_{ij}J_{ij}\vec{S}_i(\tau)\cdot\vec{S}_j(\tau)\right\}\right], \quad (36)$$

where T stands for the ordering of the τ labels and $\tilde{\epsilon}_{i\uparrow(\downarrow)}=\epsilon_i-\mu\mp h$. Now, as usual, auxiliary integrations are introduced over the variables $\vec{R}_i(\tau)$ to express the exchange term as a single-site term, to yield

$$Z_G=\exp(-\beta G)=\int \mathcal{D}R(\tau)\exp-[\Psi\{\vec{R}_i(\tau)\}], \quad (37)$$

where $\mathcal{D}R(\tau)$ stands for a functional integral (see Appendix B for the definition), and

$$\Psi\{\vec{R}_i(\tau)\}=\int_0^\beta d\tau\left(\frac{1}{2}\sum_{i,j}\rho_{ij}\vec{R}_i(\tau)\cdot\vec{R}_j(\tau)-\sum_i f_{1i}[\vec{R}_i(\tau),\epsilon_i]\right), \quad (38)$$

where the matrix $\boldsymbol{\rho}=(\mathbf{J})^{-1}$, and

$$\exp\{-f_{1i}[\vec{R}_i(\tau),\epsilon_i]\}=\mathrm{Tr}T\left\{\exp\left[\int_0^\beta d\tau\{\tilde{\epsilon}_{i\uparrow}n_{i\uparrow}(\tau)+\tilde{\epsilon}_{i\downarrow}n_{i\downarrow}(\tau)+Un_{i\uparrow}(\tau)n_{i\downarrow}(\tau)-\vec{S}_i(\tau)\cdot\vec{R}_i(\tau)\}\right]\right\}. \quad (39)$$

The one-site problem implied in Eq. (39) cannot be solved for arbitrary $\vec{R}_i(\tau)$. So we introduce a symmetry breaking assumption implying that the static fluctuations can occur only in one direction, taken to be the z-axis, i.e., we write

$$\vec{R}_i(\tau)=R_i^z\hat{k}+\vec{r}_i(\tau) \quad (40)$$

and

$$\int \vec{r}_i(\tau)d\tau=0. \tag{41}$$

Using the above assumptions, one evaluates Eq. (39) to quadratic order in $\vec{r}_i(\tau)$, which then yields the following expression for $\Psi\{\vec{R}_i(\tau)\}$ (see Appendix B):

$$\Psi\{\vec{R}_i(\tau)\}=\frac{\beta}{2}\sum_{ij}\rho_{ij}R_i^zR_j^z-\sum_i \ln\mathcal{Z}_i(h_i)$$
$$+\frac{1}{2\beta}\sum_{ij}\rho_{ij}\sum_n{}'\left(r_i^z(\omega_n)r_j^z(-\omega_n)\right.$$
$$\left.+\frac{1}{2}r_i^+(\omega_n)r_j^-(-\omega_n)+\frac{1}{2}r_i^-(\omega_n)r_j^+(-\omega_n)\right)$$
$$-\frac{1}{4}\left(\sum_{\omega_n,i}{}' r_i^-(-\omega_n)r_i^+(\omega_n)G_i(\omega_n)\right), \tag{42}$$

where $\mathcal{Z}_i$ is defined in Eq. (10) with $h_i=h+R_i^z$ replacing $(h+I_i)$, and

$$G_i(\omega_n)=\frac{2}{\mathcal{Z}_i(h_i)}\frac{\sinh(\beta h_i/2)}{i\omega_n+h_i}e^{-\beta(\epsilon_i-\mu)}, \tag{43}$$

where $\omega_n=(2\pi n)/\beta$, with n taking integer values and the prime on the n summation means exclusion of the $n=0$ term. Also

$$r_i^\alpha(\omega_n)=\frac{1}{2}\int_{-\beta}^{\beta}d\tau e^{i\omega_n\tau}r_i^\alpha(\tau) \tag{44}$$

and

$$r_i^\pm(\omega_n)=r_i^x\pm r_i^y. \tag{45}$$

With this $\Psi\{\vec{R}_i(\tau)\}$, the functional integral of Eq. (37) is evaluated by adopting a suitable generalization of the variational method due to Muhlshlegal and Zittarz.[16] In this method a quadratic trial function $\Psi_t\{\vec{R}_i(\tau)\}$ is chosen and the functional integral is evaluated in a perturbative expansion about Ψ_t. Here we choose $\Psi_t\{\vec{R}_i(\tau)\}$ to be translationally invariant. Though our problem does not have the translational symmetry, we recall that the disorder is rather weak and the homogeneity of the magnetic properties should not be much affected. This amounts to seeking a translationally symmetric quadratic form that is variationally the best for the problem. The general form for $\Psi_t\{\vec{R}_i(\tau)\}$ is

$$\Psi_t\{\vec{R}_i(\tau)\}=\frac{1}{4}\sum_{ij}\int d\tau_1\int d\tau_2\{S_{ij}^{-2}(\tau_1-\tau_2)[R_i^z(\tau_1)-a]$$
$$\times[R_j^z(\tau_2)-a]+T_{ij}^{-2}(\tau_1-\tau_2)$$
$$\times[R_i^x(\tau_1)R_j^x(\tau_2)+R_i^y(\tau_1)R_j^y(\tau_2)]\}, \tag{46}$$

where S_{ij}^{-2}, T_{ij}^{-2}, and a are the variational functions to be determined, a is later identified to be the local internal field related to the magnetization as $a=J_0m$. In Appendix B we describe the calculation of G to the first order in $(\Psi-\Psi_t)$ and the determination of the variational parameters from the resulting expression. The result of this calculation yields the following expression for the free energy G:

$$G=\frac{1}{2}\mathcal{N}_0J_0m^2-\frac{1}{\beta}\sum_i\overline{\ln\mathcal{Z}_i(J_0m)}+\frac{1}{\beta}\sum_q\sum_n{}'\ln\left(1-\frac{1}{2}\beta J_q\overline{G_0(\omega_n)}\right)+\frac{1}{2\beta}\sum_q\ln\left[1-\frac{J_q}{\beta J_0^2}\left\{\frac{1}{\mathcal{N}_0}\sum_i\overline{\ln\mathcal{Z}_i''(J_0m)}\right.\right.$$
$$\left.\left.+\sum_n{}'\overline{G_0''(\omega_n)T(\omega_n)}\right\}\right]+\frac{1}{2\beta}\sum_q\left[1-\frac{J_q}{\beta J_0^2}\left\{\frac{1}{\mathcal{N}_0}\sum_i\overline{\ln\mathcal{Z}_i''(J_0m)}+\sum_n{}'\overline{G_0''(\omega_n)T(\omega_n)}\right\}\right]^{-1} \tag{47}$$

with

$$J_q=\sum_j e^{i\vec{q}\cdot\vec{R}_{ij}}J(R_{ij}),\quad G_0(\omega_n)=\frac{1}{\mathcal{N}_0}\sum_i G_i(\omega_n),$$

and the horizontal bar over certain terms implies the following averaging:

$$\overline{f(J_0m)}=\frac{1}{2\pi}\int dy e^{-y^2/2}f(J_0m+ys). \tag{48}$$

The double prime stands for the double derivative with respect to m and

$$T(\omega_n)=\sum_q\frac{\beta J_q}{1-(1/2)\beta J_q\overline{G_0(\omega_n)}}. \tag{49}$$

These equations involve m and s, which are determined from the following equations:

$$m=\frac{1}{\beta J_0}\frac{1}{\mathcal{N}_0}\left[\sum_i\frac{\overline{\mathcal{Z}_i'(J_0m)}}{\mathcal{Z}_i(j_0m)}\right.$$
$$\left.+\frac{\partial}{\partial m}\sum_q\sum_n{}'\ln\left(1-\frac{1}{2}\beta J_q\overline{G_0(\omega_n)}\right)\right] \tag{50}$$

and

$$s^2=\frac{1}{\beta\mathcal{N}_0}\sum_k J_k\Bigg[1-\frac{J_k}{\beta J_0^2}\Bigg\{\frac{1}{\mathcal{N}_0}\sum_i \overline{\ln\mathcal{Z}_i(J_0m)''} + \sum_n{}' \overline{G_0''(\omega_n)}T(\omega_n)\Bigg\}\Bigg]^{-1}. \tag{51}$$

The above two equations are a rather formidable set of self-consistent equations which to our knowledge have not been solved even for the simpler system like the Heisenberg Hamiltonian, so here we limit the discussion to some physical effects in the low-temperature limit. On examining Eq. (47) for G, we note that the first two terms would correspond to the mean-field approximation but for the Gaussian averaging over the internal fields implied by Eq. (48). The third term corresponds to the spin-wave contribution, again corrected by fluctuations over internal fields. The last two terms are the fluctuation contribution of the internal field. At low temperatures we expect the contribution due to longitudinal fluctuations to be small on physical grounds. So if we neglect these, which amounts to neglecting the last two terms of Eq. (47) and setting $s=0$, one arrives at the following expression for G:

$$G=\frac{1}{2}\mathcal{N}_0J_0m^2-\frac{1}{\beta}\sum_i \ln\mathcal{Z}_i(J_0m) + \frac{1}{\beta}\sum_q \ln\left[\frac{1-e^{-\beta\omega_q}}{1-e^{-\beta(h+J_0m)}}\right], \tag{52}$$

where the last term here is the result of the frequency summation in the third term of Eq. (48), and

$$\omega_q=h+m[J_0-J_q] \tag{53}$$

which is the usual spin-wave frequency in the random -phase approximation. Within this approximation the equation determining the magnetization takes the form,

$$m=\frac{1}{\mathcal{N}_0}\sum_i \frac{\sinh\beta(h+J_0m)/2}{[e^{\beta(\epsilon_i-\mu)}+2\cosh\beta(h+J_0m)/2+e^{-\beta(\epsilon_i-\mu+U)}]}+\frac{1}{e^{\beta(h+J_0m)}-1}-\frac{1}{\mathcal{N}_0}\sum_q \frac{1}{e^{\beta(h+\omega_q)}-1}. \tag{54}$$

The spin-wave contribution represented by the last term yields the well-known $T^{3/2}$ term, so that Eq. (54) for $h=0$ can be written as

$$m=\int_{-W}^{W}d\epsilon g(\epsilon)\left[\frac{\sinh(\beta/2)(h+J_0m)}{e^{\beta(\epsilon-\mu)}+2\cosh(\beta/2)(h+J_0m)+e^{-\beta(\epsilon-\mu+U)}}\right]+\frac{1}{e^{\beta(h+J_0m)}-1}-\zeta(3/2)\left\{\frac{k_BT}{4\pi Dm}\right\}^{3/2}, \tag{55}$$

where D is the coefficient of q^2 in the small-q expansion of $J_0-J_q\simeq Dq^2$.

The second term is again contributing terms of the order of $\exp(-\beta J_0)$ which are insignificant at low temperatures. So one can write the solution of Eq. (55) as

$$m(T)=m_{\mathrm{MF}}(T)-\zeta(3/2)\left[\frac{k_BT}{4\pi Dm_{\mathrm{MF}}(0)}\right]^{3/2}, \tag{56}$$

where $m_{\mathrm{MF}}(T)$ is the mean-field solution whose plots have been exhibited in Fig. 4. This result is exactly what one would expect because spin-wave contributions occur in both the itinerant and local models. Here, however, much like the itinerant situation, the spin-wave contribution can be quite weak as part of the band of spin-wave excitations can become degenerate to the single-particle spin-flip excitation continuum. Note that the spin-up band is singly occupied for $(U+J_0m)/2\geqslant\epsilon\geqslant-(U+J_0m)/2$, and the spin-down band is empty at $T=0$. Thus the single-particle spin-flip excitations whose energy is $\epsilon_i-\epsilon_j+J_0m$ will span an energy range of 0 to $U+2J_0m$, which clearly engulfs the spin-wave band. The corresponding situation for itinerant magnets is that the single-particle excitations lie between between $J_0m+(1/2m)(q^2+2k_Fq)$ and $J_0m+(1/2m)(q^2-2k_Fq)$, but here the momentum selection rule saves the spin-wave excitations, as for small q there is a window for which no single-particle excitations exist. In the present situation, since the single-particle excitations are not characterized by momentum, the existence of such a window is not clear. Thus one can expect only a rather weak contribution from spin-wave excitations.

V. DISCUSSIONS

In this paper, we have presented a model for the magnetism of cluster compounds. Here both spin-flip and single-particle excitations play important roles in determining the magnetic behavior. The main results derived within the mean-field approximation, are in broad agreement with the experimental behavior. These are (i) the high field saturation magnetization corresponds to one electron moment per cluster, whereas spontaneous magnetization even at zero temperature corresponds to the nonintegral moment and is considerably smaller than the saturation magnetization. (ii) Similarly the moment inferred from high-temperature susceptibility measurements is different from the saturation magnetization. (iii) The susceptibility shows a behavior which is a mixture of localized and itinerant behavior. (iv) The calculated Arrott plots have shapes that are much like the experimental plots, showing a pronounced curvature even at low fields which is indicative of departure from the theory of weak itinerant magnets. (v) The specific heat shows a contribution linear in temperature, both below and

above the transition temperature, which is doubtless due to single-particle excitations. On the other hand, it shows a large jump at the transition temperature, which is a characteristic of localized models. (vi) We have also worked out the spin-wave excitations in the model. However since the spin-wave branch overlaps strongly with the particle-hole excitation spectrum, their contribution to the thermodynamics are not clear cut. Experimentally also, the specific heat data show possibly only a weak $T^{3/2}$ term.

Now we turn to quantitative comparisons to the data. Unfortunately data available on any one compound are not enough to verify all the quantitative features. We have attempted to obtain a fit for the compound $GaMo_4Se_8$. From the transport measurement on pure and zinc doped GaV_4S_8, we estimate a bandwidth of 1 eV. Assuming this to be true also for $GaMo_4Se_8$, one can use the expressions for T_C, and the specific heat jump at the transition temperature ΔC, to obtain the parameters U and J_0. A choice of $U/W=0.45$ and $J_0/W=0.032$ yields a T_C of 26.9 K (experimental value 26.7 K) and $\Delta C=3$ J/K/mol (the experimental value being 3.75 J/K/mol). This yields a zero-temperature spontaneous magnetization of 1.6×10^3 emu/mol, against the experimental value of 5.3×10^3 emu/mol. The linear coefficient of the specific heat γ above T_C has a value of 4.0 mJ/mol K^2 in our model for the above-mentioned values of U and J_0, whereas the experimental value of $\gamma=620$ mJ/mol K^2. The agreement with the specific heat data can improve by a factor of 10 by choosing a much smaller bandwidth for these compounds, $W=0.1$ eV, for which the γ in the paramagnetic phase ~30 mJ/mol K^2, for $U/W=0.4$ and $J_0/W=0.325$.

Though the qualitative shapes of the Arrott plots are like the experimental ones, the scales of the magnetization and the fields are off by factors of order 10. The calculated susceptibility is lower than the measured value by a factor of 8 to 10. Thus the quantitative comparisons leave much to be desired. Some of the discrepancies can be ascribed to the uncertainties regarding the bandwidth and the density of states. We have done all our calculations with a rather smooth DOS, whereas preliminary band structure calculations indicate that the DOS is rather spiky. Also the bandwidth involved in the transport measurements may be different from those entering thermodynamic properties, as localized electrons are involved here. There may also be genuine physical interactions which affect these properties, but are not included in this model. These are (a) long range Coulomb interactions and associated correlations which, for instance, give rise to the Coulomb gap; (b) disorder effects which cause variations in the on-site Coulomb interactions U and the exchange parameter J_0, and (c) degeneracy of the bands. In fact, preliminary computer simulations of this model, incorporating positional disorder effects, seem to indicate that the magnetization would differ from that estimated in our calculations. Finally, we have not understood the agency causing electron localization, which is possibly a combination of the weak disorder, long range Coulomb interactions and dispersion of bands in a few directions only. A further understanding of these should clearly improve the model. Some of these questions should be taken up especially when more extensive and precise data become available.

ACKNOWLEDGMENTS

We gratefully acknowledge the help from Professor D. D. Sarma, who calculated the band structure of a cluster compound at our request and made the preliminary results available to us. We are also grateful to Professor S. D. Mahanti for very useful discussions. S.L. acknowledges financial assistance from the University Grants Commission of India.

APPENDIX A: CHEMICAL POTENTIAL

Since the site occupation is not affected by the exchange term, the calculation of the chemical potential can be done without the exchange term. Under these circumstances, the number of particles per site, $n=N/\mathcal{N}_0$, is given by

$$n=2\int_{-W}^{W}d\epsilon g(\epsilon)\times\left[\frac{\cosh(\beta h/2)e^{-\beta(\epsilon-\mu)}+e^{-\beta(2\epsilon+U-2\mu)}}{[1+2e^{-\beta(\epsilon-\mu)}\cosh(\beta h/2)+e^{-\beta(2\epsilon+U-2\mu)}]}\right]. \tag{A1}$$

Recalling that $\int d\epsilon g(\epsilon)=1$, we can write Eq. (A1), for $n=1$, in the form

$$\int_{-W}^{W}d\epsilon g(\epsilon)\times\left[1-\frac{2\cosh(\beta h/2)e^{-\beta(\epsilon-\mu)}+2e^{-\beta(2\epsilon+U-2\mu)}}{1+2\cosh(\beta h/2)e^{-\beta(\epsilon-\mu)}+e^{-\beta(2\epsilon+U-2\mu)}}\right]=0 \tag{A2}$$

which can be further written as

$$\begin{aligned}\int_{-W}^{W}d\epsilon g(\epsilon)&\left[\frac{e^{\beta(\epsilon-\mu)}}{e^{\beta(\epsilon-\mu)}+2\cosh(\beta h/2)+e^{-\beta(\epsilon+U-\mu)}}\right]\\&=\int_{-W}^{W}d\epsilon g(\epsilon)\left[\frac{e^{-\beta(\epsilon+U-\mu)}}{e^{\beta(\epsilon-\mu)}+2\cosh(\beta h/2)+e^{-\beta(\epsilon+U-\mu)}}\right]\\&=\int_{-W}^{W}d\epsilon g(\epsilon)\left[\frac{e^{\beta(\epsilon-U+\mu)}}{e^{\beta(\epsilon-U+\mu)}+2\cosh(\beta h/2)+e^{-\beta(\epsilon+\mu)}}\right]\end{aligned} \tag{A3}$$

where in writing the last equation we have changed variables from ϵ to $-\epsilon$ and made use of the fact that $g(\epsilon)=g(-\epsilon)$. From Eq. (A3) it is clear that the equation is satisfied if $\mu=U-\mu$.

APPENDIX B: FUNCTIONAL METHOD

We start with Eq. (36) of Sec. IV. This can be written in terms of the matrix ρ and f_{1i} defined in Eq. (39) as

$$Z_G = T\Bigg[\int \mathcal{D}\vec{R}(\tau)\exp\Bigg(-\int d\tau \sum_{ij}\frac{\rho_{ij}}{2}\vec{R}_i(\tau)\cdot\vec{R}_j(\tau) - \sum_i f_{1i}[\vec{R}_i(\tau),\epsilon_i]\Bigg)\Bigg], \tag{B1}$$

where $\mathcal{D}\vec{R}(\tau)$ stands for the functional integration

$$\mathcal{D}R(\tau) = T\prod_{n=0}^{L}\prod_{i=1}^{N}\frac{\Delta^3 dR_i^x(\tau_n)dR_i^y(\tau_n)dR_i^z(\tau_n)}{(2\pi)^{3N/2}(\det J)^{3/2}} \tag{B2}$$

with $\Delta=\beta/L$, $\tau_n = n\Delta$.

Because of the quantum nature of the problem, the trace in Eq. (39) cannot be calculated exactly for any arbitrary $\vec{R}_i(\tau)$. So we introduce the symmetry breaking assumption implied in Eqs. (40) and (41). With these we can write Eq. (39) as

$$\exp[-f_{1i}] = \mathrm{Tr}T\exp\Bigg\{-\int_0^\beta d\tau[H_{0i}+V_{Ii}(\tau)]\Bigg\}, \tag{B3}$$

where

$$H_{0i} = \tilde{\epsilon}_{i\uparrow}n_{i\uparrow}(\tau) + \tilde{\epsilon}_{i\downarrow}n_{i\downarrow}(\tau) + Un_{i\uparrow}(\tau)n_{i\downarrow}(\tau) - S_i^z R_i^z \tag{B4}$$

and

$$V_{Ii}(\tau) = -[r_i^z(\tau)S_i^z(\tau) + \tfrac{1}{2}\{r_i^+(\tau)S_i^-(\tau) + r_i^-(\tau)S_i^+(\tau)\}]. \tag{B5}$$

The idea of this decomposition is to obtain f_{1i} in a perturbation expansion in $V_{Ii}\tau$. Thus

$$\exp[-f_{1i}] = \mathcal{Z}_i(h_i)\Bigg\langle T\exp\Bigg(-\int_0^\beta d\tau V_{Ii}(\tau)\Bigg)\Bigg\rangle_0, \tag{B6}$$

where $\langle\rangle_0$ indicates averaging with the density matrix $\exp(-\beta H_{0i})$ and $\mathcal{Z}_i$ has been defined earlier in Eq. (10), with $h_i = h + R_i^z$. Further

$$V_{Ii}(\tau) = e^{\tau H_{0i}}V_I(\tau)e^{-\tau H_{0i}} = -r_i^z(\tau)S_i^z - \tfrac{1}{2}\{r_i^+(\tau)e^{\tau h_i}S_i^- + r_i^-(\tau)e^{-\tau h_i}S_i^+\}. \tag{B7}$$

The first order term of the perturbation term expansion in V_{Ii} vanishes, and the second-order term yields

$$\frac{1}{2}\int_0^\beta d\tau_1\int_0^\beta d\tau_2\langle T[V_I(\tau_1)V_I(\tau_2)]\rangle = \frac{1}{8}\int_0^\beta d\tau_1\int_0^\beta d\tau_2\{r_i^+(\tau_1)r_i^-(\tau_2)G_i(\tau_1,\tau_2) + r_i^-(\tau_1)r_i^+(\tau_2)G_i(\tau_2,\tau_1)\}, \tag{B8}$$

where

$$G_i(\tau_1,\tau_2) = \langle T[S_i^-(\tau_1)S_i^+(\tau_2)]\rangle_0 = \frac{1}{\mathcal{Z}_i(h_i)}e^{-\beta(\epsilon_i-\mu)}e^{(\tau_1-\tau_2)h_i}\{\theta(\tau_1-\tau_2)e^{-\beta h_i/2} + \theta(\tau_2-\tau_1)e^{\beta h_i/2}\}. \tag{B9}$$

Keeping terms up to the second order in $\vec{r}_i(\tau)$, one can write the grand canonical free energy $G(T,\mu)$ in the following expression:

$$Z_G = \exp(-\beta G) = \int \mathcal{D}R(\tau)\exp-[\Psi\{\vec{R}_i(\tau)\}], \tag{B10}$$

where $\Psi\{\vec{R}_i(\tau)\}$ is expressed in Eq. (42). To evaluate the functional integrals of Eq. (B10) a suitable generalization of the the variational method due to Muhlschlegal and Zittarz[16] has been adopted. The quadratic trial function $\Psi_t\{\vec{R}_i(\tau)\}$ given in Eq. (46) is chosen and Eq. (B10) is evaluated in a perturbation expansion about $\Psi\{\vec{R}_i(\tau)\}$. To the first order in $[\Psi\{\vec{R}_i(\tau)\} - \Psi_t\{\vec{R}_i(\tau)\}]$ the free energy G can be written as

$$\beta G = \beta G_t + \langle\Psi\{\vec{R}_i(\tau)\} - \Psi_t\{\vec{R}_i(\tau)\}\rangle_t, \tag{B11}$$

where

$$\exp(-\beta G_t) = \int \mathcal{D}R(\tau)\exp[-\Psi_t\{\vec{R}_i(\tau)\}] \tag{B12}$$

and the averaging is done with respect to $\Psi_t\{\vec{R}_i(\tau)\}$. Since $\Psi_t\{\vec{R}_i(\tau)\}$ is translationally invariant, a more convenient form of $\Psi_t\{\vec{R}_i(\tau)\}$ can be obtained by making the following change of variables. First we replace $\vec{r}_i(\tau)$ by the Fourier transform defined as

$$\vec{r}_q(\tau) = \frac{1}{\sqrt{\mathcal{N}_0}}\sum_i e^{i\vec{q}\cdot\vec{\mathcal{R}}_i}\vec{r}_i(\tau), \tag{B13}$$

where $\vec{\mathcal{R}}_i$ denotes the coordinates of the site. The static variables R_i^z are changed to y_i by the following equation:

$$R_i^z = a + \sum_j s_{ij}y_j, \tag{B14}$$

where

$$s_{ij}^{-2} = \frac{1}{2\beta}\int_0^\beta d\tau_1\int_0^\beta d\tau_2 S_{ij}^{-2}(\tau_1-\tau_2) \tag{B15}$$

and the Fourier transformed variational parameters are defined through

$$s_{ij}^{-2}(\omega_n) = \frac{1}{2\beta}\int_{-\beta}^\beta S_{ij}^{-2}(\tau)e^{-i\omega_n\tau} \tag{B16}$$

and similarly for $T_{ij}(\tau)$. In terms of these variables

$$\Psi_t\{\vec{R}_i(\tau)\}=\frac{\beta}{2}\sum_i\ y_i^2+\frac{1}{4}\sum_q\ \sum_n{}'\left[\frac{|r_q^z(\omega_n)|^2}{s_q(\omega_n)^2}+\frac{[|r_q^x(\omega_n)|^2+|r_q^y(\omega_n)|^2]}{t_q(\omega_n)^2}\right]. \tag{B17}$$

The prime on the summation implies the exclusion of the $\omega_n=0$ term. The trial free energy G_t, apart from an unimportant constant, is given by

$$G_t=-k_BT\sum_q\ \left[\ln s_q(0)+\sum_{\omega_n}{}'\ \{\ln s_q(\omega_n)+2\ln t_q(\omega_n)\}\right], \tag{B18}$$

where s_q is the spatial Fourier transform of s_{ij} defined in Eq. (B15). Next we have to evaluate the expectation value of $\Psi\{\vec{R}_i(\tau)\}-\Psi_t\{\vec{R}_i(\tau)\}$, which in terms of the above variables can be written as

$$\Psi\{\vec{R}_i(\tau)\}-\Psi_t\{\vec{R}_i(\tau)\}=\frac{\beta}{2}\sum_{ij}\ \rho_{ij}\left(a+\sum_{ik}\ s_{ik}y_k\right)\left(a+\sum_{jl}\ s_{jl}y_l\right)-\frac{\beta}{2}\sum_i\ y_i^2-\sum_i\ \ln\Bigg[1+2e^{-\beta(\epsilon_i-\mu)}\times\cosh\frac{\beta}{2}\left(h+a+\sum_k\ s_{ik}y_k\right)+e^{-\beta(2\epsilon_i+U-2\mu)}\Bigg]+\frac{1}{2}\sum_q\ \sum_n{}'\ \Bigg[\left(\frac{\rho_{q_1q_2}}{\beta}-\frac{1}{2s_{q_1}^2}\delta_{q_1q_2}\right)r_{q_1}^z(\omega_n)r_{-q_2}^z\times(-\omega_n)+\left(\frac{1}{\beta}\rho_{q_1q_2}-\frac{1}{2t_{q_1}^2(\omega_n)}\delta_{q_1q_2}-\frac{1}{2}G_{q_1q_2}\right)\{r_{q_1}^x(\omega_n)r_{-q_2}^x(-\omega_n)+r_{q_1}^y(\omega_n)r_{-q_2}^y(-\omega_n)\}\Bigg], \tag{B19}$$

where

$$\rho_{q_1,q_2}=\frac{1}{\mathcal{N}_0}\sum_{i,j}\ \rho_{ij}\exp[i(\vec{q}_1\cdot\vec{\mathcal{R}}_i-\vec{q}_2\cdot\vec{\mathcal{R}}_j)], \tag{B20}$$

$$G_{q_1,q_2}(\omega_n)=\frac{1}{\mathcal{N}_0}\sum_i\ G_i(\omega_n)\exp[i(\vec{q}_1-\vec{q}_2)\cdot\vec{\mathcal{R}}_i)], \tag{B21}$$

where G_i is as in Eq. (43), with $h_i=h+a+\Sigma_j s_{ij}y_j$. Using the above expressions, Eq. (B19), one can evaluate the free energy G in the approximation given in Eq. (B11) to be

$$G=\frac{\rho_{0,0}\mathcal{N}_0a^2}{2}-\frac{1}{\beta}\sum_q\ \ln\frac{s_q(0)}{\beta}-\frac{1}{\beta}\sum_{q,\omega_n}{}'\ \left\{\ln\frac{s_q(\omega_n)}{\beta}+2\ln\frac{t_q(\omega_n)}{\beta}\right\}-\frac{1}{\beta}\overline{\ln\mathcal{Z}_i}+\frac{1}{2\beta^2}\sum_q\ [s_q(0)^2\rho_{q,q}-\beta/2]+\frac{1}{2\beta^2}\sum_{\omega_n,q}\ [\rho_{q,q}s_q(\omega_n)^2-\beta/2]+\frac{1}{\beta^2}\sum_{\omega_n,q}\ [\rho_{q,q}t_q(\omega_n)^2-\beta/2\overline{G_0(\omega_n)}t_q^2-\beta/2] \tag{B22}$$

where the upper bar represents the averaging of quantities which involve the variables $\{y_i\}$, in the following way:

$$\overline{f(a)}=\int\ f\left(a+\sum_k\ s_{ik}y_k\right)\exp\left(-\frac{\beta}{2}\sum_i\ y_i^2\right)\prod_i\ \sqrt{\frac{\beta}{2\pi}}dy_i=\frac{1}{\sqrt{2\pi}}\int\ dye^{-y^2/2}f(a+ys), \tag{B23}$$

where

$$s^2=\frac{1}{\beta\mathcal{N}_0}\sum_q\ s_q^2. \tag{B24}$$

Next, we determine the variational parameters by minimizing G with respect to them. The following equations are obtained:

$$s_q^2(\omega_n)=\beta J_q, t_q^2(\omega_n)=\frac{\beta J_q}{1-\frac{\beta}{2}J_q\overline{G_0}}, \tag{B25}$$

where $J_q=(\rho_{q,q})^{-1}$. Writing $a=J_0m$, one finds that the site-averaged magnetization, m, obeys the equation

$$m=\frac{1}{\beta\mathcal{N}_0}\sum_i\ \frac{\overline{\mathcal{Z}_i'(J_0,m)}}{\mathcal{Z}_i(J_0,m)}+\frac{1}{\mathcal{N}_0\beta J_0}\frac{\partial}{\partial m}\sum_q\ \sum_n{}'\ \ln\left(1-\frac{1}{2}\beta J_q\overline{G_0(\omega_n)}\right). \tag{B26}$$

y_i' denotes the derivative of y_i with respect to m. Finally, for s_k's, we have

$$s_k^2=\frac{J_k}{1-(J_k^2/\beta J_0^2)\left[\frac{1}{\mathcal{N}_0}\sum_i \overline{\ln \mathcal{Z}_i(J_0 m)''+\sum_n G_0''(\omega_n)T(\omega_n)}\right]}, \tag{B27}$$

where

$$T(\omega_n)=\frac{1}{\mathcal{N}_0}\sum_q t^2(q,\omega_n). \tag{B28}$$

For the RHS of Eq. (B27), Eq. (B25) and Eq. (B26) involve only the quantity s, one can reduce the number of entangled self-consistent equations to just two, those determining m and s^2, the equation for s^2 being

$$s^2=\frac{1}{\mathcal{N}_0\beta}\sum_k J_k\left[1-\frac{J_k}{\beta J_0^2}\left(\frac{1}{\mathcal{N}_0}\sum_i \overline{\ln \mathcal{Z}_i(J_0 m)''+\sum_n{}' \overline{G_0''(\omega_n)}T(\omega_n)}\right)\right]^{-1}. \tag{B29}$$

The substitution of these parameters in Eq. (B22) leads to the G given in Eq. (47).

[1] H. Barz, Mater. Res. Bull. **8**, 983 (1973).

[2] A. Simon, Angew. Chem. Int. Ed. Engl. **20**, 1 (1983).

[3] J. M. Vandenberg and D. Brasen, J. Solid State Chem. **14**, 203 (1975).

[4] C. Perrin, R. Chevrel and M. Sergent, C. R. Hebd. Seances Acad. Sci. C, Sci. Chim. **280**, 949 (1975).

[5] Y. Sahoo and A. K. Rastogi, J. Phys. Condens. Matter **5**, 5953 (1993).

[6] Y. Sahoo and A. K. Rastogi, Physica B **275**, 233 (1995).

[7] A. K. Rastogi, in *Current Trends in Physics of Materials*, edited by M. Youssouf (World Scientific, Singapore, 1987).

[8] A. K. Rastogi, A. Berton, J. Chaussy, R. Tournier, H. Patel, R. Chevrel, and M. Sergent, J. Low Temp. Phys. **52**, 539 (1983).

[9] T. A. Kaplan, S. D. Mohanti, and W. Hartman, Phys. Rev. Lett. **27**, 1796 (1971).

[10] H. Kamimura, in *The Metal-Nonmetal Transition in Disordered Systems*, edited by E. R. Friedman and D. P. Tunstall (SUSSP, Edinburgh, 1978), p. 327; H. Kamimura, in *Proceedings of the 14th International Conference on Physics of Semiconductors*, edited by B. L. H. Wilson (The Institute of Physics, Bristol, 1978), p. 981.

[11] H. Kamimura and E. Yamaguhci, Solid State Commun. **28**, 127 (1978).

[12] D. D. Sarma (private communication).

[13] H. Kamimura, in *Electron-Electron Interactions in Disordered Systems*, edited by A. L. Efros and M. Pollack (North-Holland, Amsterdam, 1985), p. 666. This reference is a review of the work done by Kamimura and co-workers.

[14] In fact, as intercluster distances decrease in S as compared to Se compounds this kinetic exchange contribution seems to increase. However, ferromagnetism dominates especially at low temperatures.

[15] D. M. Edwards and E. P. Wohlfarth, Proc. R. Soc. London, Ser. A **303**, 127 (1968).

[16] B. Muhlschlegal and J. Zittarz, Z. Phys. **175**, 553 (1963).

[17] R. Micnas, Physica A **98**, 403 (1979).

[18] V. G. Vaks, A. I. Larkin, and S. A. Pikin, Zh. Eksp. Teor. Fiz. **53**, 281 (1967) [Sov. Phys. JETP **53**, 1089 (1967)].

[19] Z. Onyszkiewicz, Phys. Lett. A **57A**, 480 (1976).